

## 3D HYDRODYNAMICAL SIMULATIONS OF STELLAR SURFACES : APPLICATIONS TO *GAIA*

Bigot, L. & Thévenin, F.<sup>1</sup>

### Abstract.

We use 3D time-dependent hydrodynamical simulations to model the photospheres of late type stars in a very realistic way. We apply these simulations to study the 3D line formation in the spectral domain of the spectrometer on board in the space mission *Gaia*.

### 1 Introduction

The *Gaia* space mission (Perryman et al. 2001) will provide an unprecedented opportunity to map the actual chemical composition of million of stars throughout the Milky Way. Knowing the distances thanks to the astrometric instrument, the photometer on board will provide the fundamental stellar parameters such as the effective temperature, gravity and average metallicity. The Radial Velocity Spectrometer (RVS) will allow a determination of the chemical abundances by observing individual spectral lines (Katz et al. 2004, Wilkinson et al. 2005). Collecting these stellar abundances, it will be then possible to map of the chemical composition of our Galaxy for million of stars (up to  $V=12-13$ ), i.e. to a scale never reached before. The knowledge of this chemical composition of the Galaxy from the disk to the halo will provide information on its formation and history. Regarding the importance of the mission and its goals, it is mandatory to have the best models to extract the physical parameters of the observed stars. It is worth mentioning that these abundances are *not* observed but *interpret* through models. The model atmospheres must therefore be as realistic as possible. The convection plays an essential role in the line forming process and deeply influences the shape, shift and asymmetry of lines in late type stars which will represent most of the stars that will be observed by *Gaia*. To date, most of the abundance determinations are done in 1D *hydrostatic* models in LTE or NLTE. These models have difficulties to fit the shape of the observed lines and more important they require the use of adjustable parameters such as the micro and macro turbulence which are used to mimic the effects of the convection. This is an important source of uncertainties in the diagnostic. This problem can be avoided by using 3D radiative hydrodynamical (RHD) models that naturally account for turbulent motions. Another important aspect of the 3D RHD simulations is that they can correct the convective shifts (few hundreds m/s) of the lines which has to be subtracted to the global lineshifts when determining the stellar radial velocities. A realistic modelling of stellar atmospheres is therefore crucial for a better interpretation of future data.

In this paper, we present preliminary work which consists in using state-of-the-art 3D RHD simulations to calculate synthetic line profiles in the wavelength region of *Gaia*/RVS. We first focus on the Ca II triplet and then discuss the use of these models to derive accurate radial velocities, corrected from convective lineshifts.

### 2 The 3D modelling of the stellar atmospheres

Realistic modelling of the solar and stellar surfaces has been developed since the early eighties by Nordlund and coworkers (Nordlund 1982, Stein & Nordlund 1989, Nordlund & Dravins 1990, Stein & Nordlund 1998, Asplund et al. 2000). They found great success in reproducing observed constraints such as granulation topology, spectral lines, helioseismic data. In the present work, we use a code that solves the equations for mass, momentum and internal energy in a conservative form, for fully 3D compressible flow on a staggered mesh (Nordlund &

---

<sup>1</sup> Université Nice Sophia Antipolis, Observatoire de la Côte d'Azur, BP 4229, 06304, Nice cedex 4

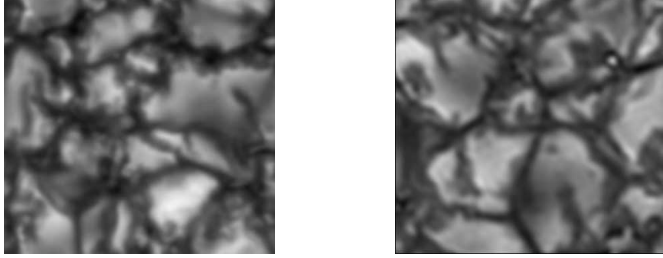


**Fig. 1.** Comparison between synthetic disk-center emergent intensity (left panel) and the observed equivalent (Right panel) made at the Solar Swedish Telescope (SST). Each panel represents an area of  $6000 \times 6000$  kms. (Left) Synthetic image obtained by a 3D RHD simulation (Bigot, unpublished) with a grid resolution of  $512^2 \times 384$  (11.6 kms horizontal). The synthetic image is smoothed by an Airy function that mimics the PSF of the SST. (Right) G-band (4305 Å) image obtained at the SST using adaptative optics and speckle reconstruction. This image (unpublished) is kindly provided by J. Hirzberger. Data of the same observations may be found in Wiehr et al. (2004) and Hirzberger & Wiehr (2005). The resolution is  $0.041''$  (30kms).

Galsgaard 1995). The code uses 6th order finite differences and 5th order interpolation. The time advance is done by a 3rd order Runge-Kutta scheme. Horizontal boundary conditions are periodic whereas top and bottom boundary conditions are transmitting. We use ghost zones at the top and the bottom of the domain in order to use the same spatial derivative scheme at the boundaries and in the interior. The code is stabilized by numerical diffusion of the Von Neumann and Richtmyer type in the momentum and energy equations. The Uppsala's equation-of-states and opacities are used (Gustafsson et al. 1975 + updates). The radiative transfer is solved by using wavelength binning technique (Nordlund 1982).

Each model is defined by the entropy at the bottom of the simulation domain, the gravity and the chemical composition. We note that the effective temperature is not an input in our model but rather an output fluctuating around a mean value. For each stellar model, the time sequence spans several hours, enough to cover several convective turn-overs. An illustration of the realism of the 3D RHD simulation is shown in Fig. 1.

In order to calculate synthetic spectra, we extract from the 3D RHD simulation a run of about 1 hour, with snapshots stored every 10 min. For each of them, the radiative line transfer was solved with long characteristics using a Feautrier scheme. Pure LTE (no scattering) is assumed. We use the most recent quantum mechanical calculations of hydrogen collisions with neutral species (Barklem & O'Mara 1997, Barklem et al. 1998) to account for Van der Waals broadening. This is a great improvement compared with the traditional Unsöld recipe since we no longer need an enhancement factor. The disk-center or disk-integrated intensities are computed for each grid point at the surface. The 2D time-dependent surface intensity profiles are then spatially and temporally averaged before comparison with observations.

### 3 Applications to *Gaia*/RVS

There are several advantages to use 3D RHD simulations in stellar abundance and radial velocity determinations. These simulations lead to a very good fit of the observed lines in shape, depth, shifts and asymmetry as shown by Asplund and coworkers in a series of papers (e.g. Asplund et al. 2000, 2004) and by Bigot & Thévenin (2006) for the RVS spectral domain. Moreover, on the contrary to hydrostatic models, the 3D hydrodynamical ones naturally account for turbulent motions and therefore do not need the use of the traditional micro and macro turbulence. These adjustable quantities, which are unavoidable in 1D hydrostatic models, lead to some uncertainties in the diagnostic of stellar parameter determinations, in particular for abundance determinations.

Another important advantage is the possibility to calculate the convective shifts of the spectral lines. These shifts are of the order of a few hundreds m/s to a few km/s for late type stars. Since the RVS aims at determining the stellar radial velocities ( $V_{\text{rad}}$ ) of the Galaxy, it is particularly important to use these simulations to subtract the doppler shifts coming from the hydrodynamic motions *inside* the star. The precision expected for *Gaia*/RVS will be of the order of 1km/s (up to  $V=15$  depending on spectral type).

In the following sections we apply these 3D hydrodynamical simulations to two cases of interest for *Gaia*/RVS which are the fit of the Ca II triplet and the convective shift correction for radial velocity determination.

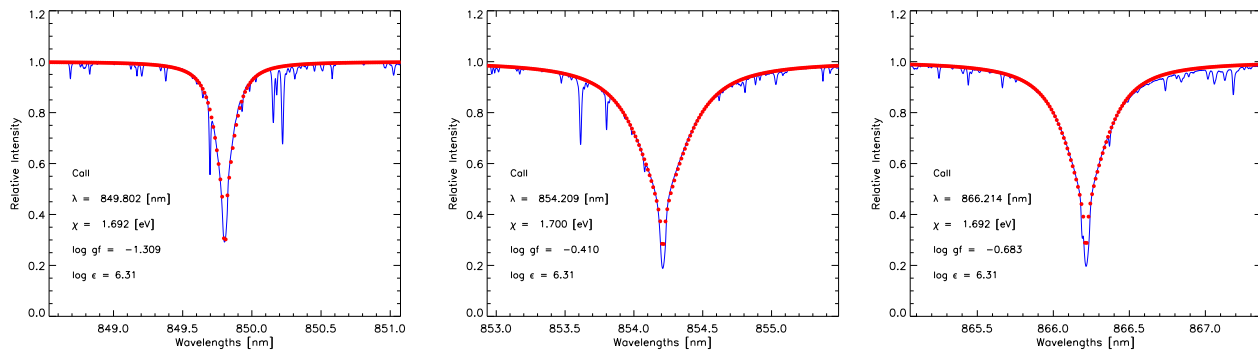


**Fig. 2.** Fits of the synthetic (●) disk-center Ca II triplet with solar spectrum (full line). The central depression is not well fitted since the line cores are formed in non-LTE conditions.

### 3.1 The calcium II triplet

The RVS spectral domain has been chosen mainly for the presence of the calcium II triplet ( $\lambda = 849.802, 854.209, 866.214$  nm). This strong triplet will be visible in most stars, even in metal poor stars. We then pay a special attention to the calculation of synthetic profiles for these three lines (Bigot & Thévenin, 2008). In this work, we decided to fit the solar Ca II triplet by fixing the abundance of calcium ( $[Ca/H]=6.31$ ) and by adjusting the oscillator strengths ( $\log gf$ ) whose values provided by database such as VALD (Kupka et al. 1999) are often badly known. The fit of these three lines is shown in Fig. 2. For such simulations we used a grid resolution of  $253^2 \times 163$ . The synthetic profiles were convolved with a Gaussian function representing the instrumental profile of the solar FTS ( $\lambda/\delta\lambda \approx 500000$ ). The calculated profiles are shifted to take into account the gravitational redshift (633 m/s). Since the core of these lines is formed in the chromosphere and might suffer from NLTE effects, we only fit the wings of the Ca II triplet. The derived values (-1.309, -0.410, -0.683) are very close to quantum mechanical calculation of Meléndez et al. (2007) : -1.356 , -0.405, -0.668, respectively. This good agreement, without adjustable parameters, is in favor of the realism of our simulations.

### 3.2 The convective shift corrections

The primary goal of the RVS is to determine the radial velocities of stars. In order to have an accurate  $V_{\text{rad}}$ , one must correct the contribution of the convective shift. The amplitude of these lineshifts depends on the location of the formation of the line and on the star itself. We calculate a series of line profiles for different stars :  $\alpha$  Cen B (K dwarf), sun and  $\alpha$  Cen A (G dwarfs), Procyon (F star) and the metal poor star HD 84937. For this work, we used in all cases a grid resolution of  $128^2 \times 96$ . An investigation of convective shifts for late type stars was first made by Dravins & Nordlund (1990) but with a much lower resolution than ours. We focus for this exercise on the Ca II triplet and Fe I lines. The latter were selected to be non blended lines and to cover the spectral domain of the RVS (Bigot & Thévenin 2006).

As seen in Fig. 3ab the Fe I lines are blueshifted. This is due to the fact that they are formed deeply into the atmosphere where most of the light is emitted from the bright ascending granules. This is the case of most of the Fe I lines of our sample, with some exceptions like Fe I 868.86 nm. The convective shifts for Fe I lines range from a few hundreds m/s for  $\alpha$  Cen B up to about 1 km/s for Procyon. The amplitude of the shift increases when going from K dwarfs to earlier type star such as Procyon, as a consequence of the more vigorous convective motions :  $V_{\text{rms}} = 1.4$  km/s for  $\alpha$  Cen B and 4.1 km/s for Procyon.

As seen in Fig. 3c the Ca II triplet lines are redshifted. This is a consequence of the fact that these lines are formed well above the photosphere ( $\tau < 0.1$ ). This is an overshoot region where the granulation is reversed: The largest fluctuations of temperature correspond to the descending flows (see e.g. Cheung et al. 2004 for a numerical investigation of this property.). The amplitude of the convective shift is larger than for Fe I lines.

## 4 Conclusion

The 3D RHD simulations are very helpful for the stellar abundance and radial velocity determinations. The main advantage lies in the fact that these simulations reproduce the stellar surfaces with a great realism. Since

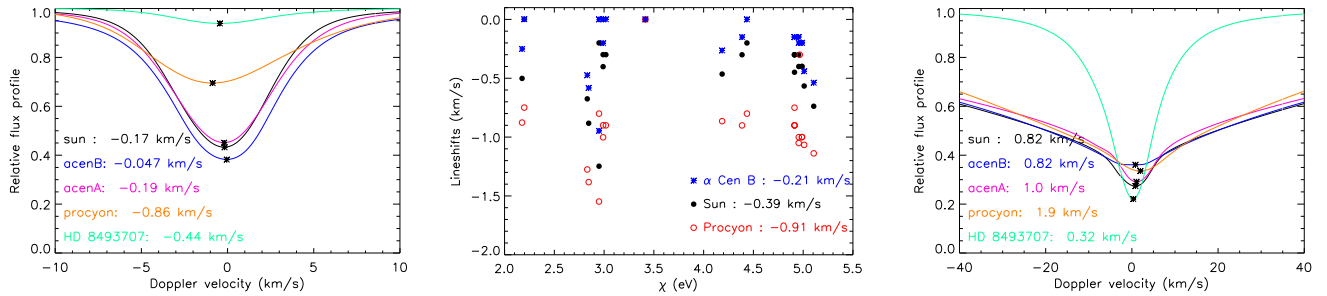


**Fig. 3.** (Left) Flux profiles of the Fe I at 851.407 nm for different stars. The lineshifts are indicated in each case. (Middle) Convective blueshifts of some Fe I lines of interest for the RVS (Bigot & Thévenin, 2006) as function of the excitation potential for three different stars:  $\alpha$  Cen B, the Sun and Procyon. The convective shift increases as the star is hotter. (Right) The same as left panel but for the Ca II line at 854.209 nm. In that case, the convection leads to a redshift.

all the dynamics is naturally taken into account, they do not need to use adjustable free parameters that generally pollute the diagnostics in stellar physics. We have shown that these simulations can be useful for *Gaia*/RVS to get accurate line profiles and even more important for the RVS they allow corrections of the convective shifts to the determination of radial velocities. The amplitude of these lineshifts for late type stars can be of the order of the accuracy expected for the radial velocities, i.e.  $\sim 1$  km/s. In a future work, we will explore these corrections to more stars throughout the HR diagram.

## Acknowledgments

We thank Å. Nordlund for providing his code. L. Bigot thanks the organizers of the session "Action Spécifique Gaia" for the invitation to present this work during the "Journées de la SF2A 2008".

## References

- Asplund, M., Nordlund, Å., Trampedach, R., Allende Prieto, C., & Stein, R. F. 2000, *A&A*, 359, 729  
 Asplund, M., Grevesse, N., Sauval, A. J., Allende Prieto, C., & Kiselman, D. 2004, *A&A*, 417, 751  
 Barklem, P. S., & O'Mara, B. J. 1997, *MNRAS*, 290, 102  
 Barklem, P. S., O'Mara, B. J., & Ross, J. E. 1998, *MNRAS*, 296, 1057  
 Bigot, L., & Thévenin, F. 2006, *MNRAS*, 372, 609  
 Bigot, L., & Thévenin, F. 2008, *Journal of Physics Conference Series*, in press  
 Cheung, M. C. M., Schessler, M., & Moreno-Insertis, F. 2004, *A&A*, 461, 1163  
 Dravins, D., & Nordlund, Å. 1990, *A&A*, 228, 184  
 Dravins, D., & Nordlund, Å. 1990, *A&A*, 228, 203  
 Gustafsson, B. et al. 1975, *A&A*, 42, 407  
 Hirzberger, J., & Wiehr, E. 2005, *A&A*, 438, 1059  
 Katz, D., Munari, U., Cropper, M., Zwitter, T., Thévenin, F., David, M., Viala, Y., et al. 2004, *MNRAS*, 354, 1223  
 Kupka, F., Piskunov, N., Ryabchikova, T. A., Stempels, H. C., & Weiss, W. W. 1999, *A&AS*, 138, 119  
 Meléndez, M., Bautista, M. A., & Badnell, N. R. 2007, *A&A*, 469, 1203  
 Nordlund, Å. 1982, *A&A*, 107, 1  
 Nordlund, Å., & Dravins, D. 1990, 228, 155  
 Nordlund, Å., & Galsgaard, K. 1995, <http://www.astro.ku.dk/> kg  
 Perryman, M. A. C., de Boer, K. S., Gilmore, G., Hög, E., Lattanzi, M. G., et al. 2001, *A&A*, 369, 339  
 Stein, R.F., & Nordlund, Å. 1989, *ApJ*, 342, L95-98  
 Stein, R.F., & Nordlund, Å. 1998, *ApJ*, 499, 914  
 Wiehr, E., Bovelet, B., & Hirzberger, J. 2004, *A&A*, 422, L63  
 Wilkinson, M. I., Vallenari, A., Turon, C., Munari, et al. 2005, 359, 1306.